Journal of Thermal Analysis and Calorimetry (2020) 140:1935–1944
https://doi.org/10.1007/s10973-019-08945-8

Energy and economic analysis of evaporative vacuum easy desalination system with brine tank

H. Kariman[1] · S. Hoseinzadeh[2,3] · A. Shirkhani[3] · P. S. Heyns[2] · J. Wannenburg[2]

Received: 12 July 2019 / Accepted: 18 October 2019 / Published online: 2 November 2019

Abstract

Nowadays, the freshwater is one of the most critical issues for humans. In this regard, desalination systems can be beneficial. In this research, at first different types of desalination systems and their governing equations is studied. Then the energy consumption of evaporative vacuum easy desalination system with brine tank is modeled. This modeling and the equations governing the energy consumption of new subsets such as the evaporator, condenser, vacuum pump, and other pumps are presented. In the end, the economic modeling of the system is investigated. The feasibility of using the system is reported in three cities (Abu Dhabi, Las Palmas, and Perth). The results shown that the annual operating cost of the pumps is estimated to be 0.19 M€ yr^{-1}, 0.51 M€ yr^{-1} and 0.14 M€ yr^{-1} for Abu Dhabi and Las Palmas and Perth respectively. Also, the annual cost of fresh water production is compared with other reaches in these cities. The results are shown that Perth has the lowest cost of the fresh water output at 0.67 M€ yr^{-1} and Las Palmas has the highest cost of fresh water production with 0.104 M€ yr^{-1}. The reason is the difference in the electricity prices in these cities.

Keywords Thermal energy analysis · Desalination system · Fresh water · Vacuum pump · Economic analysis

List of symbols

A	Active surface of the heat transfer (m^2)
C_f	Heat capacity of feed water (J kg^{-1} K^{-1})
C_p	Heat capacity of the water at constant pressure (J kg^{-1} K^{-1})
C_{pl}	Heat capacity of saturated water (J kg^{-1} K^{-1})
C_{pd}	Heat capacity of distillated water (J kg^{-1} K^{-1})
C_{MED}	Cost of MED (€)
C_{cond}	Cost of condenser (€)
E	Energy need to provide hot water (w)
G	Gravity (m/s^2)
H	Average heat transfer coefficient (w M^{-2} k^{-1})
H_b	Enthalpy of brine (J kg^{-1})
H_t	Enthalpy of tank water (J kg^{-1})
H_f	Enthalpy of feed water (J kg^{-1})
H_{fg}	Heat of evaporation (J kg^{-1})
H_{fg2}	Heat capacity of the water condensation (J kg^{-1})
H_{fgg}	Corrected value of the special water heat capacity (J kg^{-1})
Ja	Jacobin coefficient
K_l	Temperature conductivity in saturated liquid state (W m^{-1} K^{-1})
L	Length (m)
M_{0b}	Brine flow rate (L h^{-1})
M_{0c}	Cooling water flow rate (L h^{-1})
M_{0f}	Feed water flow rate (L h^{-1})
M_{0h}	Heating water flow rate (L h^{-1})
$Mn_{a\text{-}cl}$	Mass of salt (g)
M_T	Tank flow (L)
AOC_{lab}	Annual operative cost of labor
$AOC_{heating\text{-}fluid}$	Annual operative cost of heating fluid (€ yr^{-1})
TAC	Total annual cost (€ yr^{-1})
Q	Heat exchanged (J s^{-1})
S	Salinity (g L^{-1})
$T_{ambient}$	Temperature of ambient (°C)
T_h	Temperature of heating water (°C)

✉ S. Hoseinzadeh
Hoseinzadeh.siamak@gmail.com;
Hosseinzadeh.siamak@up.ac.za

[1] Faculty of Mechanical and Energy Engineering, Shahid Beheshti University, Tehran, Iran

[2] Centre for Asset Integrity Management, Department of Mechanical and Aeronautical Engineering, University of Pretoria, Pretoria, South Africa

[3] Young Researchers and Elite Club, West Tehran Branch, Islamic Azad University, Tehran, Iran

T_b	Temperature of brine (°C)
T_f	Temperature of feed water (°C)
T_s	Temperature of surface (°C)
T_{sat}	Temperature of saturation (°C)

Greek letters

ρl	Density at saturated liquid (kg m^{-3})
ρv	Density at saturated vapor (kg m^{-3})
μl	Dynamic viscosity at saturated liquid (Pa s)
ΔTLMTD	Logarithmic temperature difference (°C)

Introduction

As we know, one of the future crises of modern humanity to survive on this planet is a shortage of fresh water for consumption [1]. More than 2/3 Earth is made up of water, but unfortunately, 94% of it is the ocean and ocean water that is non-drinkable saline water [2]. Only 3% of the total freshwater of world water can be used, which is often found in polar fridges and ground springs [3]. As we have seen, the high potential of salt water in the world has led humans to sweeten this water and turn it into drinkable water. The processes of desalinating work according to the principle of energy. Which are classified into two classes; First, Temperature processes involving phase change. Second, Membrane processes, including pressure energy. Thermal processes are classified into several categories such as; multi-stage evaporation (MEE), multi-stage flash (MSF) and Compressed vapor (VC). Also, Membrane processes are classified into several categories; Reverse Osmosis (RO) and Electro Dialysis (ED) [4]. To analyze the systems of desalination, Rautenbach examined general desalination system and made it possible to use it in different scales [5]. Morin compared the multi-effect desalination and multi-stage flash systems and found some impressive results. He concluded that the multi-effect desalination system has advantages such as lower initial cost and less cost-performance, and it has fewer problems than a multi-stage flash system [6].

Rashidi et al. performed the thermodynamic analysis of the COP cycle. Also, they used the first and second law to analyze system performance and observed that there is a linear relationship between the specific heat of the operating fluid and its temperature [7, 8].

Sheikholeslami et al. focus on the effects of a magnetic field and thermal energy on hydrothermal $Fe_3O_4eH_2O$ and the $CuOeH_2O$ nanofluid. The solution of final equations obtained by CVFEM for different values of Darcy numbers (Da), and Reynolds number (Re). Also, they worked on latent heat thermal energy storage systems (LHTESS) to save thermal energy. The results show that by adding CuO nanoparticles to pure PCM, the compression process increases [9, 10]. In the other researches, three-dimensional porous cavities with magnetic field effect were investigated. They used the Lattice Boltzmann method and observed that the degree of gradient had a direct relationship with Darcy Number and Reynolds number [11–13]. He also researched CuO nanoparticles and found that using nanoparticles are an excellent way to accelerate the process of charging and full energy increasing [12, 14, 15]. He also studied on the heat transfer of the nanosilver (cooled) under thermal effect radiation researched and total energy, average temperature, isotherm, and solids [16–22].

Javadi et al. studied a mathematical model with a nominal capacity of 500 MW. This study was carried out using three-way optimization method. They also simulated a conventional hybrid cycle unit in Iran using a mathematical approach. Sensitivity analysis was performed on environmental emissions and electricity prices, exergy efficiency, CO_2 emissions, and production costs were assessed [23, 24].

Hoseinzadeh et al. [25] studied thermal energy and economic analysis of zero-energy buildings in the humid mountainous area. In this regard, a residential building was used as a typical condition. And the energy efficiency and cost parameters were investigated [26, 27]. The research method in this study is based on two principles and MATLAB software was used. According to the results, 80% of the amount of electrical energy used for air conditioning in the building and repelled from 34 to 7 MW. In the case of return on investment (R0I), the electricity needed to generate, and the cost can be about $ 15,000 a year [28–32].

The study conducted by Gonda et al. [33] was also useful to get the flat-plate flatwork. In their research, the empirical results of evaporation indicated the film of falling water on a galvanized sheet. This module has consisted of stainless steel, which has a total heat and a thermal area of 0.267 m^2 which has been tested.

Elsafi et al. [33] studied the humidification-dehumidification desalination and concentrated photovoltaic-thermal collectors and analyzed them in terms of energy and exergy-costing. Elsayed et al. [34] investigated the exergo-economic study of the MED system operating on a steam-compressor unit MED-MVC. The results showed that the production amount is 1500 m^3/day, and the efficiency of the second law is 2.8%.

Olatayo et al. [35] studied wind systems in South Africa and concluded that although much energy is wasted and cannot be used by wind turbines, small-scale wind technologies can be used alongside government programs. It is considered economical and should, therefore be evaluated for its potential use in energy and economics. The possibility of using these cysts has also been evaluated in various parts of the country, and the low efficiency and low energy produced by this technology are the reason why it has not been used and developed.

As well as Zheng et al. [36] explored the feasibility of using the wind system in New Zealand and tracked environmental risk and cost factors.

Tovar et al. [37] also examined how the food–water–and energy cycles are connected, and proposed a new policy for connecting and evaluating this cycle.

For the thermodynamic analysis of wind energy systems, Hu et al. [38] conducted an exergy and energy analysis of wind systems and investigated the effect of factors such as wind speed, pressure, temperature and humidity rate on the efficiency of the system and the results showed Although the amplitude of the wind speed affects the performance of the system, the other factors mentioned have a high impact on the performance of the system and provided the effect of these factors. Asensio1 et al. [39] Study was carried out to achieve the equations of desalination systems operating on wind energy. In this study, they investigated the economic analysis of the reverse osmosis desalination plant system, which, by adding wind energy to the system, reduced the cost of fresh water production to 0.022 EUR m^{-3}.

In order to obtain information on the use of solar and wind energy in the reverse osmosis Desalination work with Mitoa et al. [40], In this study, they examined the system's strategic, functional and control settings, and ways to demonstrate system adaptability for renewable energies.

Agha et al. [41] consider the optimization of pool size and the number of steps for three different storage area temperatures. One consequence is that excessive quantity will lead to the rejection of some heat accumulated during the summer. The sensitivity analysis of the various factors affecting water costs shows that capital costs account for about 80% of total expenses and costs of the SP/MSF will be around 13–10% [42].

Kaldellis et al. [43] investigate the economic viability of desalination. The proposed analysis of all cost parameters is considered. These costs include the initial cost of the desalination plant, the annual cost of maintenance and operation, the cost of energy consumption, the capital cost index, and the associated inflation rate. The results show that the RES-based desalination system is the most promising and sustainable method for supplying fresh water and drinking water.

Then Kavvadias et al. [44] present a method for maintaining the high standards and reliability of some economic models. Sensitivity analysis was used to identify the most critical parameters in the DEEP model. This review proves that the DEEP economic model is entirely appropriate. Nisan et al. [45] a detailed analysis of the cost and cost of water for several nuclear reactors operating in one operation is presented. It has been presented and shown in particular, how to reduce desiccant costs by the use of micro-heat.

Ejli et al. [46] presents a comparative study of water cost for three cities in southern Morocco using two desalination processes: reverse osmosis and steam compression. Sources provide energy requirements: grid and wind energy and therefore, four combinations of desalination processes are considered in the assessment of desalination cost. An economic analysis of the main effects of the parameters related to the cost of produced water level is also presented.

Choi et al. [47] presented the new economic feasibility study for several methods and the feasibility and costs of chemical treatment. In the other same work, zou et al. [48] presented Economic effects analysis of seawater desalination in China with input–output technology. In this paper, five different configurations of a seawater desalination system using photovoltaic are studied. Plus a case study of an island in Greece was investigated. The present study shows that seawater reverse osmosis with photovoltaic energy and desalination unit, which includes water storage, is a low capacity battery. Filippini et al. [49] presented Design and economic evaluation of solar-powered hybrid multi effect and reverse osmosis system for seawater desalination. In this study, the feasibility of connecting a desalination plant to a solar photovoltaic (PV) field to produce electricity at a low cost and in a sustainable manner was investigated. And a detailed mathematical model for the PV system is presented. Information on four locations, namely Isola di Pantelleria (IT), Las Palmas (ES), Abu Dhabi (United Arab Emirates) and Perth (AUS) have seen used economically. It has examined the feasibility of installing the proposed plant, especially the solar PV farm at these four locations.

In this research, after studying different types of desalination systems and governing their equations, the energy consumption evaporative vacuum easy desalination system is modeled. After modeling, the energy consumption of new subsets such as the evaporator, condenser, vacuum pump, and other new pumps are presented. Since this system is home-sized, it is instrumental. And it can be used in any part of the world that has problems with access to unsafe water. On the other hand, the economic issues governing desalination systems are studied. Especially, desalination with brain thank system that the economy of this system and It is based on the cost of water production is analyzed. In the end, the economic analysis is obtained with three important cities (Abu Dhabi, Las Palmas, and Perth) in the world, and we compared them.

Desalination system modeling

The system consists of two heat exchanger and the type of heat exchangers are plate. The amount of heat transfer of them are 0.72 m^2 and each one can be divided into two sub-sections. The first part is the heating and steam section, which consists of two heating and evaporator sections. In the cooling section, the cooling unit is consisted of two sub-sections of cooling and condenser.

The heating cell, the evaporating cell, the cooling cell and the brine tank are known as an evaporative desalination system. Also, the condenser cell and vacuum pump and the heater unit and the other pumps are each introduced separately as a system and examined in economic analysis. The schematic form of this evaporative desalination system with the vacuum brine tank is given in Fig. 1.

Each of the system subsets are described as following.

Heating system

In the heating section, the heating cell has an environmental pressure, and the hot water entering into the temperature of 70 °C has a warming effect. The required amount of heating to evaporate the water by rotating this hot water is provided

In the evaporator section, the pressure is reduced by a vacuum pump and reaches to 12 mbar that causes the evaporation temperature of the water to decrease and reaches an approximate 49.6 °C. In this section, the feeding water is entered into the brine tank at first and after mining, it is pumped into the set, the top-of-the-range distribution system supplies this entry. A portion of the water is evaporated, and it is entered into the condenser. And pump removes the amount of water that does not evaporate as brine from the set and enters into the brine tank and needs its heat into the feeding water.

Brine tank of system

In the tank, the concentration of feed water is measured in each stage after mixing with brine water by concentration gauge. This concentration gauge is connected to the brine tank next to the sewage valve. If the concentration of feed water were higher than the permitted limit, it would be removed from the system as wastewater, and if it had low salt concentration, it would re-enter into the system and run the cycle.

Cooling system

In the cooling section, the cooling unit consists of two subsections of cooling and condenser. The cooling system is provided by the tap water supply, which causes the surface temperature of the metal between two parts equal to the tap water temperature. The amount of the evaporated water in evaporator section is introduced the condenser by holes. And it is condensed on this flat metallic surface and is removed from the cell by a pump.

Vacuum pump of system

The vacuum pump is used to reduce gas pressure in a given volume, in other words, to minimize gas density. Therefore, it is necessary to remove gas particles such as air from the volume to be vacuumed. In this system, the vacuum pump reduces the pressure in the evaporator and condenser cells and the brine tank to 12 mbar. Of all types of vacuum pumps, Oily rim pumps are selected because they are suitable for water vapor and water vapor and can supply the required pressure [50, 51].

Other pumps of system

The other pumps in the system are conventional pumps that we use for such things as rotating the heating water, draining the fresh water and entering and rotating the feed water.

The values of fluid discharge in rotation within the system are presented in Table 1. Plus, the amount of fresh water produced by the system is approximately 21 L h^{-1}.

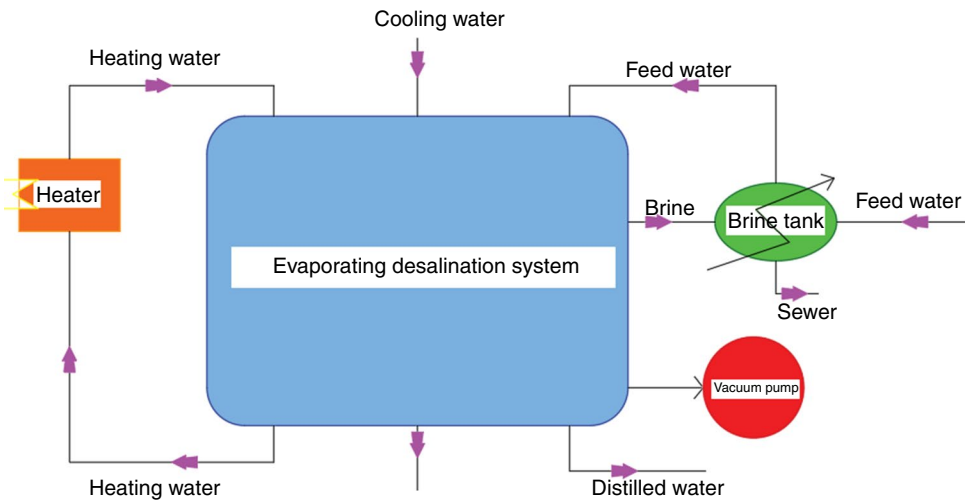

Fig. 1 Schematic of the evaporative vacuum domestic desalination system with Brine tank

Table 1 Fluid flow values in system rotation

Fluid	Amount
Heating fluid (QH)	3 $m^3\ h^{-1}$
Feed water (Qf):	150 L h^{-1}
Cooling water (Qc):	0.5–1 $m^3\ h^{-1}$

The decision parameters for modeling of the system are presented in Table 5.

After obtaining the energy consumption of each of the system subsystems, we perform a system economic analysis and obtain the governing equations of the system. The economic equations of the system are presented in Table 6. These equations are taken from paper [49].

Table 2 The energy equations governing of heater and evaporator

Description	Equation		Unit
Heater			
Maximum energy needed for heater	$E_1 = M_h^0 \times (T_h - T_{ambient})$	(1)	W
Energy needed for heater during the cycle	$E_2 = M_h^0 \times (T_{hi} - T_{ho})$	(2)	W
Evaporator			
Logarithmic temperature in evaporator	$\Delta T_{LMTD} = \frac{Thi-Tho}{Ln\frac{Thi-Tb}{Tho-Tb}}$	(3)	°C
Heat exchanged in evaporator	$Q(1) = H \times A \times \Delta T_{LMTD}$	(4)	J s^{-1}
The amount of evaporated water	$M_d^0 = \frac{(Q(1)-(M0f\times Cpf\times(Tb-Tf))}{Hfg}$	(5)	L h^{-1}

Table 3 The energy equations governing of Brine tank and condenser

Description	Equation		Unit
Brine tank			
Salinity	$S = \frac{Mna\_cl}{Mt-M^0d}$	(6)	g L^{-1}
Enthalpy balance	$H_f = H_t + H_b$	(7)	J kg^{-1}
Condenser			
Jacobin coefficient [52]	$Ja = \frac{Cpl\times(Tsat-Ts)}{Hfg_2}$	(8)	Without unit
Special water heat capacity	$Hfgg = Hfg_2 \times (1 + (0.68 \times ja))$	(9)	J kg^{-1}
Value of the heat transfer	$H_l = 0.943 \times \frac{(g\times\rho l(\rho l-\rho v)\times Hfgg\times L^3)^{0.25}}{\mu l\times Kl\times(Tsat-Ts)}$	(10)	w $M^{-2}\ k^{-1}$
Heat is transferred in cooling cell	$Q(2) = H_L \times A \times (T_{sat} - T_S)$	(11)	J s^{-1}
Distilled water	$M^0d = \frac{Q(2)}{Hfgg}$	(12)	L h^{-1}

Table 4 The energy equations governing of vacuum pump and other pump

Description	Equation		Unit
Vacuum and other pumps			
Energy consumption for vacuum pump	$\frac{1}{\tau} \times BkW = 21.4 \times (SF)^{0.924} \times \frac{1}{\tau}$	(13)	J s^{-1}
Factor efficiency	$SF = \frac{m}{P}$	(14)	kg $torr^{-1}$
The amount of mass required is log out	$M = V \times \rho air$	(15)	kg
Other pumps power	Pump power $= M^0 \times (H_{outlet} - H_{inlet})$	(16)	W
Total energy consumption of system	Etotal $= E2 +$ vacuum power + pumps power	(17)	W

Energy and economic analysis

In order to achieve the economic modeling of this system, we first obtain the energy consumption equations for each of the subsets, then present the economic equations governing the system. The energy equations governing each subset of the system are presented in Tables 2, 3, and 4.

The decision parameters for economic modeling of the system are presented in Table 7. Some of these values are taken from the paper [49].

After economic simulation and achieving the economic equations of the evaporative vacuum domestic desalination system, it is concluded that one of the most important pillars

Table 5 The decision parameters for modeling this system

Parameters	Value	Unit
C_{ph}	4181.000	J kg^{-1} K^{-1}
T_h	368.150	K
$T_{ambient}$	298.150	K
H	1100.00	w M^{-2} k^{-1}
A	0.720	m^2
T_b	347.75	K
H_{fg}	2.380×10^6	J kg^{-1}
$M_{na\text{-}cl}$	0.912	G
C_{pl}	4.170×10^3	J kg^{-1} K^{-1}
T_{sat}	348.000	K
H_{fg2}	2.380×10^6	J kg^{-1}
G	9.800	m s^{-2}
ρl	988.250	kg m^{-3}
ρv	0.080	kg m^{-3}
μl	7.240×10^{-4}	Pa s
Kl	0.622	W m^{-1} K^{-1}
L	1.800	m
C_{pd}	1.940×103	J kg^{-1} K^{-1}
V	0.720	m^3
ρair	1.225	kg m^{-3}
τ	0.800	

in economic analysis is the electricity price system since it has a vacuum pump to supply the vacuum governing the system. However, other factors such as the incoming feed water temperature and the salt concentration are also unaffected.

Table 7 The decision parameters for economic modeling of the system

Parameter	Value	Unit
THY	4380.000	h yr^{-1}
K_{intake}	43.000	€ day m^{-3}
K_{MED}	1.400	–
K_{Cond}	2.800	–
$C_{heating\ -fluid}$	0.0036	€ kg^{-1}
$C_{mat\text{-}cond}$	425.000	€ m^{-2}
$C_{mat\text{-}MED}$	3300.000	€ m^{-2}
C_{lab}	0.020	€ m^{-3}
Ir	0.070	–
Life	15.000	year

Table 8 The input variables for economic analysis

Parameters	Abu Dhabi	Las Palmas	Perth
Electricity cost (€/kWh)	0.070	0.190	0.052
Av. Seawater temperature (°C)	27.000	22.000	24.000
Av. seawater salinity (ppm)	40,000.000	35,000.000	35,000.000

The following research examines the feasibility of using this system in three locations around the world. These three points include Las Palmas. Abu Dhabi, Perth. The input variables for economic analysis at these three points are presented in Table No 8. As mentioned earlier, this system

Table 6 Economic equations of the system

Description	Equation		Unit
Fresh water cost	$\mathrm{sTAC} = \frac{\mathrm{TAC}}{\mathrm{Mfresh}\times\mathrm{THY}\times3600}$	(18)	€/m^3
Total annual cost	$\mathrm{TAC} = \mathrm{AOC} + \mathrm{CRF}\times\mathrm{TCC}$	(19)	€ yr^{-1}
Total capital cost	$\mathrm{TCC} = \mathrm{CAPEX_{dir}} + \mathrm{CAPEX_{indir}}$	(20)	€
Direct CAPEX	$\mathrm{CAPEX_{dir}} = \mathrm{CAPEX_{civil\ -\ work}} + \mathrm{CAPEX_{equipment}}$	(21)	€
Indirect CAPEX	$\mathrm{CAPEX_{indir}} = 0.25\times\mathrm{CAPEX_{dir}}$	(22)	€
Civil work cost	$\mathrm{CAPEX_{civil\ -\ work}} = 0.15\times\mathrm{CAPEX_{equipment}}$	(23)	€
Equipment cost	$\mathrm{CAPEX_{equipment}} = C_{\mathrm{MED}} + C_{\mathrm{intake}} + C_{\mathrm{cond}}$	(24)	€
Sea water pre-treatment and intake cost	$C_{\mathrm{Intake}} = \frac{K_{\mathrm{Intake}}\times12\times3600\times M_{\mathrm{seawater}}}{\rho}$	(25)	€
Final condenser cost	$C_{\mathrm{Cond}} = K_{\mathrm{Cond}}\times C_{\mathrm{mat\ -\ Cond}}\times A_{\mathrm{Cond}}^{0.8}$	(26)	€
MED system cost	$C_{\mathrm{MED}} = K_{\mathrm{MED}}\times C_{\mathrm{mat\ -\ MED}}\times A_{\mathrm{MED}}^{0.64}$	(27)	€
Annual operative cost	$\mathrm{AOC} = \mathrm{AOC_{lab}} + \mathrm{AOC_{chem}} + \mathrm{AOC_{pow}} + \mathrm{AOC_{man}} + \mathrm{AOC_{heating\ -\ fluid}}$	(28)	€ yr^{-1}
Cost of human labor	$\mathrm{AOC_{lab}} = \frac{C_{\mathrm{lab}}\times\mathrm{THY}\times100\times M_{\mathrm{fresh}}}{\rho}$	(29)	€ yr^{-1}
Cost of chemical treatment	$\mathrm{AOC_{chem}} = \frac{C_{\mathrm{chem}}\times\mathrm{THY}\times3600\times M_{\mathrm{seawater}}}{\rho}$	(30)	€ yr^{-1}
Cost of power & vacuum pump	$\mathrm{AOC_{pow}} = \frac{C_{\mathrm{pow}}\times\mathrm{THY}\times100\times M_{\mathrm{fresh}}}{\rho\times\eta}\times f(\Delta P)$	(31)	€ yr^{-1}
Cost of maintenance	$\mathrm{AOC_{man}} = 0.002\times\mathrm{TCC}$	(32)	€ yr^{-1}
Cost of heating fluid utility	$\mathrm{AOC_{heating\ -\ fluid}} = \frac{C_{\mathrm{Heating\ -\ fluid}}\times\mathrm{THY}\times(Ts-40)\times M_{\mathrm{heating\ -\ fluid}}}{80} + 0.005\times\mathrm{TCC}$	(33)	€ yr^{-1}
Capital recovery factor	$\mathrm{CRF} = \frac{Ir\times(1+Ir)^{\mathrm{life}}}{(1+Ir)^{\mathrm{life}}-1}$	(34)	1/yr

Table 9 Result of economic analysis of Abu Dhabi

Result	Value
AOC_{power}	0.191582 M€ yr^{-1}
AOC_{total}	0.259657 M€ yr^{-1}
TCC	0.406816 M€
TAC	0.719360 M€ yr^{-1}

Table 10 Result of economic analysis of Las Palmas

Result	Value
AOC_{power}	0.519895 M€ yr^{-1}
AOC_{total}	0.587970 M€ yr^{-1}
TCC	0.406816 M€
TAC	0.1047674 M€ yr^{-1}

Table 11 Result of economic analysis of Perth

Result	Value
AOC_{power}	0.142318 M€ yr^{-1}
AOC_{total}	0.210393 M€ yr^{-1}
TCC	0.406816 M€
TAC	0.670097 M€ yr^{-1}

is home-based and portable and can be provided anywhere in the world with freshwater scarcity problems if provided. If applicable, be used.

Result

Abu Dhabi

Abu Dhabi city is situated on an island in the Persian Gulf off the central western coast, while the majority of the city and Emirate reside on the mainland connected to the rest of the country. As of 2019, Abu Dhabi's urban area has an estimated population of 1.45 million people.

Abu Dhabi is one of the cities facing water problems and also has good groundwater levels and therefore has high potential to use this evaporative vacuum domestic desalination system with Brine tank. The details of this city are presented in Table 8. The economic analysis results for this city show that the cost of freshwater is equal to 0.719,360 M€ yr^{-1}. The price of other influential economic factors are reported in Table 9.

Las Palmas

Las Palmas is located in the northeastern part of the island of Gran Canaria, about 150 km off the Moroccan coast in the Atlantic Ocean. Las Palmas experiences a hot desert climate. This city also suffers from a water problem. Also. This city has the potential to use evaporative vacuum domestic desalination system with brine tank. The details of this city are presented in Table 8.

The results of economic analysis for the city show that the cost of fresh water is equal to 0.1047674 M€ yr^{-1}.

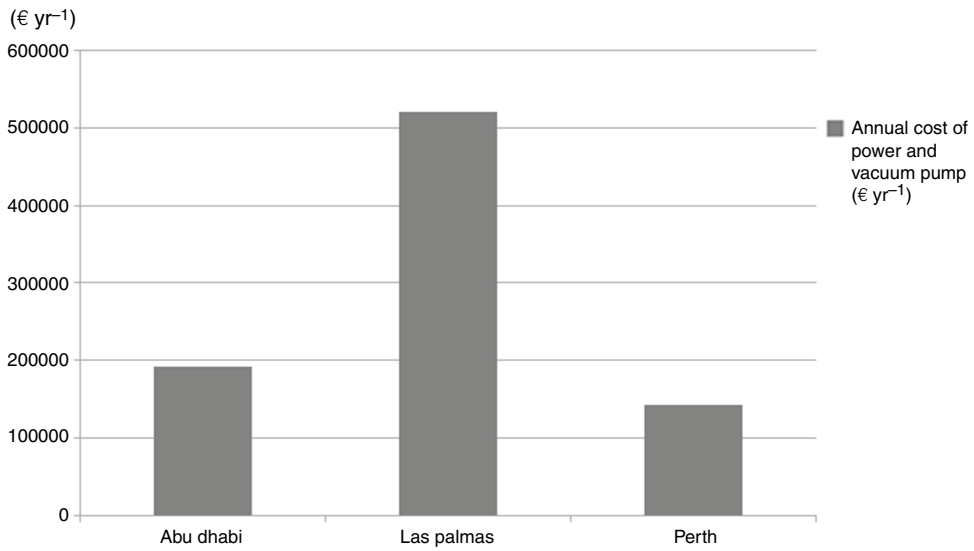

Fig. 2 Annual cost of power & vacuum pump

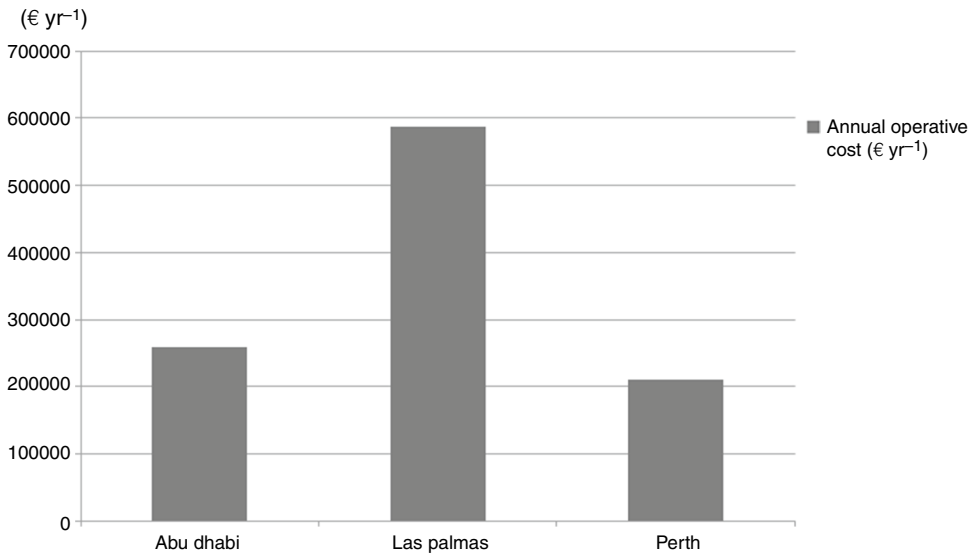

Fig. 3 The annual operating cost

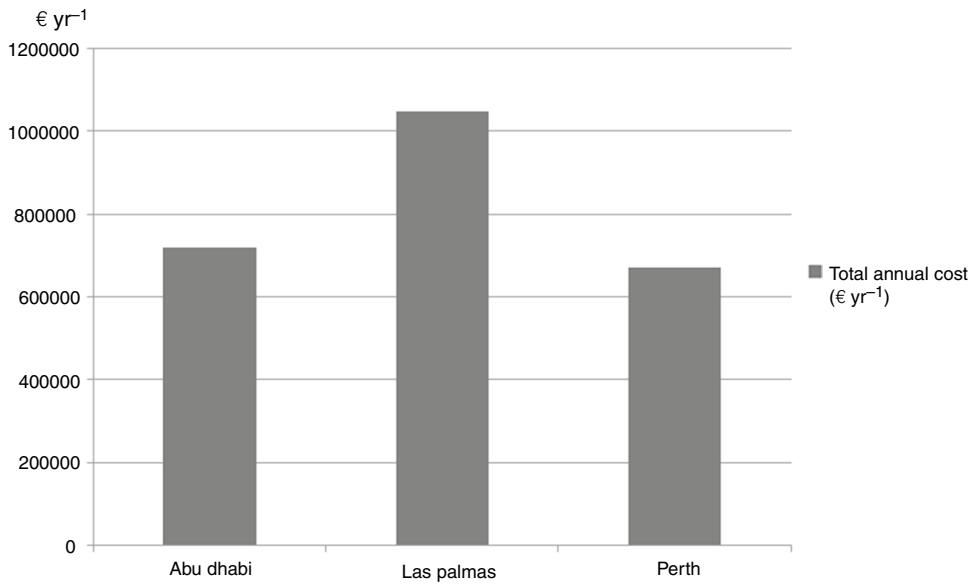

Fig. 4 The total annual cost

Costs other effective economic factors are reported in Table 10.

Perth

Perth is part of the South West Land Division of Western Australia, with the majority of the metropolitan area located on the Swan Coastal Plain, a narrow strip between the Indian Ocean and the Darling Scarp. The first areas settled were on the Swan River at Guildford, with the city's central business district and port (Fremantle) both later founded downriver. This city also suffers from a water problem and has the potential to use evaporative vacuum domestic desalination system. The details of this city are presented in Table 8.

The results of economic analysis for the city show that the cost of fresh water is equal to 0.670097 M€ yr^{-1}. Costs other practical economic factors are reported in Table 11.

Besides, to compare the cost of using this system in different cities, the following diagrams are presented. Figure 2 shows the annual operating cost amount used to generate electricity in pumps (conventional pumps and vacuum pumps). This figure is presented to compare these three cities. The cost of generating electricity at pumps covers a large proportion of annual operating expenses. This system has a

vacuum pump which has to supply the vacuum of the system and therefore has high power consumption.

As can be seen in Fig. 2, Las Palmas has the highest electricity cost for pump use, which is due to the high cost of electricity in the city. Perth has the lowest cost of pumps because it has the lowest electricity cost. On the other hand, Fig. 3 compares the annual operating cost of the desalination system in these three cities. As can be seen in Fig. 3, Las Palmas has the highest annual operating cost. Also, Fig. 4 is presented to compare the final annual cost of fresh water production by this evaporative desalination system in these three cities

As shown in Figs. 2–4, it can be recognized that Perth and Abu Dhabi are less costly to produce fresh water than the Las Palmas. This fact indicates that this new easy desalination system can be used and cost-effective because of the low cost of electricity in these cities.

Conclusions

In this study, complete modeling of the new evaporative vacuum easy desalination system with brine tank was introduced. All components and sub-systems such as pumps are modeled. In terms of energy consumption, the economic feasibility of the system is examined. So, the economic equations of this system and its components were presented. Three critical cities provided the following information from different parts of the world (Abu Dhabi, Las Palmas, and Perth) with different characteristics. The results have shown that the annual operating cost of the pumps was estimated to be 0.19 M€ yr^{-1}, 0.51 M € yr^{-1} and 0.14 M€ yr^{-1} for Abu Dhabi and Las Palmas and Perth respectively.

Additionally, the annual cost of fresh water production is compared with each other in the three cities. The results is confirmed that Perth had the lowest cost of fresh water production at 0.67 M€ yr^{-1}. Las Palmas has the highest cost of fresh water production at 0.104 M€ yr^{-1}. The reason is the difference in electricity prices in these two cities.

References

1. El-Dessouky H, Alatiqi I, Bingulac S, Ettouney H. Steady-state analysis of the multiple effect evaporation desalination process. Chem Eng Technol Ind Chem Plant Equip Process Eng Biotechnol. 1998;21(5):437–51.
2. Ali MB, Kairouani L. Multi-objective optimization of operating parameters of a MSF-BR desalination plant using solver optimization tool of Matlab software. Desalination. 2016;381:71–83.
3. Malik SN, Bahri PA, Vu LT. Steady state optimization of design and operation of desalination systems using Aspen Custom Modeler. Comput Chem Eng. 2016;91:247–56.
4. Bandi CS, Uppaluri R, Kumar A. Global optimization of MSF seawater desalination processes. Desalination. 2016;394:30–43.
5. Rautenbach R. Progress in distillation. Desalination. 1993;93(1–3):1–13.
6. Morin OJ. Design and operating comparison of MSF and MED systems. Desalination. 1993;93(1–3):69–109.
7. Mousapour A, Hajipour A, Rashidi MM, Freidoonimehr N. Performance evaluation of an irreversible Miller cycle comparing FTT (finite-time thermodynamics) analysis and ANN (artificial neural network) prediction. Energy. 2016;94:100–9.
8. Rashidi MM, Parsa AB, Shamekhi L, Nazari F, Ali M. Exergetic optimisation of a multi-stage compression transcritical refrigeration cycle. Int J Exergy. 2016;20(1):22–47.
9. Sheikholeslami M. Solidification of NEPCM under the effect of magnetic field in a porous thermal energy storage enclosure using CuO nanoparticles. J Mol Liq. 2018;263:303–15.
10. Sheikholeslami M. Numerical simulation for solidification in a LHTESS by means of Nano-enhanced PCM. J Taiwan Inst Chem Eng. 2018;86:25–41.
11. Sheikholeslami M. Finite element method for PCM solidification in existence of CuO nanoparticles. J Mol Liq. 2018;265:347–55.
12. Sheikholeslami M, Shamlooei M. Fe_3O_4–H_2O nanofluid natural convection in presence of thermal radiation. Int J Hydrog Energy. 2017;42(9):5708–18.
13. Sheikholeslami M. Application of Darcy law for nanofluid flow in a porous cavity under the impact of Lorentz forces. J Mol Liq. 2018;266:495–503.
14. Sheikholeslami M, Ghasemi A. Solidification heat transfer of nanofluid in existence of thermal radiation by means of FEM. Int J Heat Mass Transf. 2018;123:418–31.
15. Sheikholeslami M. Numerical modeling of nano enhanced PCM solidification in an enclosure with metallic fin. J Mol Liq. 2018;259:424–38.
16. Sheikholeslami M, Zeeshan A. Analysis of flow and heat transfer in water based nanofluid due to magnetic field in a porous enclosure with constant heat flux using CVFEM. Comput Methods Appl Mech Eng. 2017;320:68–81.
17. Sheikholeslami M, Vajravelu K. Nanofluid flow and heat transfer in a cavity with variable magnetic field. Appl Math Comput. 2017;298:272–82.
18. Sheikholeslami M, Darzi M, Sadoughi MK. Heat transfer improvement and pressure drop during condensation of refrigerant-based nanofluid; an experimental procedure. Int J Heat Mass Transf. 2018;122:643–50.
19. Sheikholeslami M. Influence of magnetic field on Al2O3-H2O nanofluid forced convection heat transfer in a porous lid driven cavity with hot sphere obstacle by means of LBM. J Mol Liq. 2018;263:472–88.
20. Sheikholeslami M, Rokni HB. Melting heat transfer influence on nanofluid flow inside a cavity in existence of magnetic field. Int J Heat Mass Transf. 2017;114:517–26.
21. Sheikholeslami M, Sheremet MA, Shafee A, Li Z. CVFEM approach for EHD flow of nanofluid through porous medium within a wavy chamber under the impacts of radiation and moving walls. J Therm Anal Calorim. 2019;138(1):573–81. https://doi.org/10.1007/s10973-019-08235-3.
22. Farshad SA, Sheikholeslami M. Simulation of exergy loss of nanomaterial through a solar heat exchanger with insertion of multichannel twisted tape. J Therm Anal Calorim. 2019;138(1):795–804. https://doi.org/10.1007/s10973-019-08156-1.
23. Javadi MA, Hoseinzadeh S, Khalaji M, Ghasemiasl R. Optimization and analysis of exergy, economic, and environmental of a combined cycle power plant. Sādhanā. 2019;44(5):121.
24. Javadi MA, Hoseinzadeh S, Ghasemiasl R, Heyns PS, Chamkha AJ. Sensitivity analysis of combined cycle parameters on exergy,

economic, and environmental of a power plant. J Therm Anal Calorim. 2019; 1–7.
25. Hoseinzadeh S, Heyns PS, Chamkha AJ, Shirkhani A. Thermal analysis of porous fins enclosure with the comparison of analytical and numerical methods. J Therm Anal Calorim. 2019;138(1):727–35. https://doi.org/10.1007/s10973-019-08203-x.
26. Hoseinzadeh S, Moafi A, Shirkhani A, Chamkha AJ. Numerical validation heat transfer of rectangular cross-section porous fins. J Thermophys Heat Transf. 2019;33:698–704.
27. Hoseinzadeh S, Sahebi SAR, Ghasemiasl R, Majidian AR. Experimental analysis to improving thermosyphon (TPCT) thermal efficiency using nanoparticles/based fluids (water). Eur Phys J Plus. 2017;132(5):197.
28. Hoseinzadeh S. Thermal performance of electrochromic smart window with nanocomposite structure under different climates in Iran. Micro Nanosyst. 2019;11(2):154–64.
29. Hoseinzadeh S, Hadi Zakeri M, Shirkhani A, Chamkha AJ. Analysis of energy consumption improvements of a zero-energy building in a humid mountainous area. J Renew Sustain Energy. 2019;11(1):015103.
30. Hoseinzadeh S, Azadi R. Simulation and optimization of a solar-assisted heating and cooling system for a house in Northern of Iran. J Renew Sustain Energy. 2017;9(4):045101.
31. Yousef Nezhad ME, Hoseinzadeh S. Mathematical modelling and simulation of a solar water heater for an aviculture unit using MATLAB/SIMULINK. J Renew Sustain Energy. 2017;9(6):063702.
32. Yari A, Hosseinzadeh S, Golneshan AA, Ghasemiasl R. Numerical simulation for thermal design of a gas water heater with turbulent combined convection. In: ASME/JSME/KSME 2015 joint fluids engineering conference. American Society of Mechanical Engineers Digital Collection; 2015.
33. Gonda A, Lancereau P, Bandelier P, Luo L, Fan Y, Benezech S. Water falling film evaporation on a corrugated plate. Int J Therm Sci. 2014;81:29–37.
34. Elsafi AM. Integration of humidification-dehumidification desalination and concentrated photovoltaic-thermal collectors: energy and exergy-costing analysis. Desalination. 2017;424:17–26.
35. Olatayo KI, Wichers JH, Stoker PW. Energy and economic performance of small wind energy systems under different climatic conditions of South Africa. Renew Sustain Energy Rev. 2018;98:376–92.
36. Gu W, Wang X, Wang L, Yin X, Liu H. Performance investigation of an auto-tuning area ratio ejector for MED-TVC desalination system. Appl Therm Eng. 2019;155:470–9.
37. Serrano-Tovar T, Suárez BP, Musicki A, Juan A, Cabello V, Giampietro M. Structuring an integrated water-energy-food nexus assessment of a local wind energy desalination system for irrigation. Sci Total Environ. 2019;689:945–57.
38. Hu W, Liu Z, Tan J. Thermodynamic analysis of wind energy systems. In: Wind solar hybrid renewable energy system. IntechOpen; 2019.
39. Rosales-Asensio E, Borge-Diez D, Pérez-Hoyos A, Colmenar-Santos A. Reduction of water cost for an existing wind-energy-based desalination scheme: a preliminary configuration. Energy. 2019;167:548–60.
40. Mito MT, Ma X, Albuflasa H, Davies PA. Reverse osmosis (RO) membrane desalination driven by wind and solar photovoltaic (PV) energy: state of the art and challenges for large-scale implementation. Renew Sustain Energy Rev. 2019;112:669–85.
41. Agha KR. The thermal characteristics and economic analysis of a solar pond coupled low temperature multi stage desalination plant. Sol Energy. 2009;83(4):501–10.
42. El-Dessouky HT, Ettouney HM. Fundamentals of salt water desalination. Amsterdam: Elsevier; 2002.
43. Kaldellis JK, Kavadias KA, Kondili E. Renewable energy desalination plants for the Greek islands—technical and economic considerations. Desalination. 2004;170(2):187–203.
44. Kavvadias KC, Khamis I. The IAEA DEEP desalination economic model: a critical review. Desalination. 2010;257(1–3):150–7.
45. Nisan S, Dardour S. Economic evaluation of nuclear desalination systems. Desalination. 2007;205(1–3):231–42.
46. Ejli D, Benchrifa R, Bennouna A, Zazi K. Economic analysis of wind-powered desalination in the south of Morocco. Desalination. 2004;165:219–30.
47. Choi S, Kim B, Nayar KG, Yoon J, Al-Hammadi S, Han J, Al-Anzi B. Techno-economic analysis of ion concentration polarization desalination for high salinity desalination applications. Water Res. 2019;155:162–74.
48. Zou Q, Liu X. Economic effects analysis of seawater desalination in China with input–output technology. Desalination. 2016;380:18–28.
49. Filippini G, Al-Obaidi MA, Manenti F, Mujtaba IM. Design and economic evaluation of solar-powered hybrid multi effect and reverse osmosis system for seawater desalination. Desalination. 2019;465:114–25.
50. Boxman RL, Sanders DM, Martin PJ, editors. Handbook of vacuum arc science and technology: fundamentals and applications. Norwich: William Andrew; 1996.
51. Lewin G, Russell AM. Fundamentals of vacuum science and technology. Am J Phys. 1965;33:977.
52. Bergman TL, Incropera FP, DeWitt DP, Lavine AS. Fundamentals of heat and mass transfer. New York: Wiley; 2011.